

Biophysical Controls on Light Response of Net CO₂ Exchange in a Winter Wheat Field in the North China Plain

Xiaojuan Tong^{1*}, Jun Li^{2*}, Qiang Yu^{3,2}, Zhonghui Lin²

1 College of Forestry, Beijing Forestry University, Beijing, China, **2** Key Laboratory of Water Cycle and Related Land Surface Processes, Institute of Geographic Science and Natural Resources Research, Chinese Academy of Sciences, Beijing, China, **3** Plant Functional Biology and Climate Change Cluster, University of Technology, Sydney, Australia

Abstract

To investigate the impacts of biophysical factors on light response of net ecosystem exchange (NEE), CO₂ flux was measured using the eddy covariance technique in a winter wheat field in the North China Plain from 2003 to 2006. A rectangular hyperbolic function was used to describe NEE light response. Maximum photosynthetic capacity (P_{\max}) was $46.6 \pm 4.0 \mu\text{mol CO}_2 \text{ m}^{-2} \text{ s}^{-1}$ and initial light use efficiency (α) $0.059 \pm 0.006 \mu\text{mol} \mu\text{mol}^{-1}$ in April–May, two or three times as high as those in March. Stepwise multiple linear regressions showed that P_{\max} increased with the increase in leaf area index (LAI), canopy conductance (g_c) and air temperature (T_a) but declined with increasing vapor pressure deficit (VPD) ($P < 0.001$). The factors influencing P_{\max} were sorted as LAI, g_c , T_a and VPD. α was proportional to $\ln(\text{LAI})$, g_c , T_a and VPD ($P < 0.001$). The effects of LAI, g_c and T_a on α were larger than that of VPD. When $T_a > 25^\circ\text{C}$ or $\text{VPD} > 1.1\text{--}1.3 \text{ kPa}$, NEE residual increased with the increase in T_a and VPD ($P < 0.001$), indicating that temperature and water stress occurred. When g_c was more than 14 mm s^{-1} in March and May and 26 mm s^{-1} in April, the NEE residuals decline disappeared, or even turned into an increase in g_c ($P < 0.01$), implying shifts from stomatal limitation to non-stomatal limitation on NEE. Although the differences between sunny and cloudy sky conditions were unremarkable for light response parameters, simulated net CO₂ uptake under the same radiation intensity averaged 18% higher in cloudy days than in sunny days during the year 2003–2006. It is necessary to include these effects in relevant carbon cycle models to improve our estimation of carbon balance at regional and global scales.

Citation: Tong X, Li J, Yu Q, Lin Z (2014) Biophysical Controls on Light Response of Net CO₂ Exchange in a Winter Wheat Field in the North China Plain. PLoS ONE 9(2): e89469. doi:10.1371/journal.pone.0089469

Editor: Ben Bond-Lamberty, DOE Pacific Northwest National Laboratory, United States of America

Received: June 1, 2012; **Accepted:** January 23, 2014; **Published:** February 20, 2014

Copyright: © 2014 Tong et al. This is an open-access article distributed under the terms of the Creative Commons Attribution License, which permits unrestricted use, distribution, and reproduction in any medium, provided the original author and source are credited.

Funding: This research is jointly supported by National Natural Science Foundation of China (Grant No. 31100322), National Basic Research Program of China (Grant No. 2010CB428404 and Grant No. 2012CB955304) and the Fundamental Research Funds for the Central Universities (NO.YX2011-19). The funders had no role in study design, data collection and analysis, decision to publish, or preparation of the manuscript.

Competing Interests: The authors have declared that no competing interests exist.

* E-mail: tongxjsxbs@sina.com (XT); lijun@igsnr.ac.cn (JL)

Introduction

Vegetation productivity is the foundation of carbon sequestration and grain yield formation. For the limit on field observation techniques, early studies mainly focused on photosynthesis at the leaf level. The biochemistry and ecophysiology of leaf photosynthesis have been well understood and parameterized [1,2]. However, it is difficult to measure leaf photosynthesis over long periods and upscale photosynthetic rate from the leaf level to the canopy or ecosystem level because of the non-linear distribution of leaf area and radiation intensity within the vegetation canopy. With the development of micrometeorological techniques, especially the eddy covariance (EC) method, net photosynthetic rate of vegetation could be directly measured at the ecosystem level. The EC technique has been widely used in CO₂ flux measurements in forest, grassland and farmland ecosystems [3–9].

Plant photosynthesis is primarily driven by incident solar radiation. Light response models, including rectangular hyperbolic model [10,11] and non-rectangular hyperbolic model [12,13], were developed to describe the relationship between daytime net ecosystem CO₂ exchange (NEE) and photosynthetically active

radiation (PAR). Besides solar radiation, factors influencing daytime NEE include environmental variables such as air temperature, vapor pressure deficit and soil water content and biological variables such as leaf area index and canopy conductance. These factors may be considered by (1) estimating the bias of simulated NEE as functions of influencing factors [14,15], or (2) revising light response parameters as functions of influencing factors [9,11,16–19]. The effects of biophysical factors on light response parameters are often estimated using stepwise multiple linear regression models [9]. However, these models have not been used to assess the influence of variables on NEE residual so far.

Long-term observations and simulations have shown a worldwide decrease in surface solar radiation (global dimming) from 1950s to 1980s, with a partial recovery (brightening) in 1990s in some areas (e.g. high and middle latitude of the Northern Hemisphere) [20]. During the dimming period, direct radiation declined remarkably, whereas diffuse radiation enhanced. The increase in diffuse fraction of surface solar radiation may be attributed to increasing aerosol and/or cloudiness, as both factors tend to enhance scattering in the atmosphere [20]. Light responses of photosynthesis under various sky conditions were investigated in

forests [8,21–23] and croplands [24,25]. For the tall and dense vegetations, photosynthesis may be enhanced by diffuse radiation because diffuse light distributes more effectively within the canopy compared with direct light [26]. After considering the effects of direct and diffuse radiation on canopy photosynthesis in the model, Mercado et al. [27] found that the increases in diffuse fraction enhanced the global land carbon sink by 23.7% during the period from 1960 to 1999.

China is the largest wheat producer and consumer in the world [28] and continuously attempts to increase its production to ensure national food security. As one of large food production regions in China, the North China Plain (NCP) produces about half of the country's wheat [29]. In this study, CO₂ flux was measured continuously using the EC technique in a winter wheat field in the North China Plain for 4 years. The objectives are to (1) investigate NEE light response and the influencing factors, and (2) assess the effects of sky conditions on NEE light response. This study will improve our knowledge on the parameterization of carbon cycle models and the scenario analyses of carbon sink in the future under changing climate.

Materials and Methods

Study site

This study was conducted at Yucheng Comprehensive Experiment Station, Chinese Academy of Sciences (36°57'N, 116°38'E, 23.4 m). It is located at the North China Plain, with a temperate monsoon climate. Mean annual temperature is 13.1°C and annual solar radiation is 5242 MJ m⁻². Annual precipitation is about 528 mm. Soil organic content is 1.21% and pH value is about 7.9. The typical cropping system in this region is the biannual rotation with winter wheat and summer maize. In this study, winter wheat was planted in mid/late October and harvested in early/mid June. The detailed field management was described by Tong et al. [30].

Field observations

CO₂ and latent heat fluxes were measured by the eddy covariance system with a three-dimensional sonic anemometer (model CSAT3, Campbell Sci. Inc., USA) and an infrared open-path CO₂/H₂O gas analyzer (model LI-7500, Li-Cor Inc., USA). The eddy covariance system, mounted at the height of 2.1 m, was used to measure 3-D wind speed, air temperature, humidity and CO₂ concentration above the canopy. Raw data were collected at 10 Hz and recorded by a CR5000 datalogger (model CR5000, Campbell Scientific Inc., USA). The CR5000 datalogger can store data and programs on a PC card. The card can be carried to a computer and the computer reads PC cards via its PCMCIA card slot directly.

Anemometers (model A100R, Vector, UK) and psychrometers (model HMP45C, Vaisala, Finland) were installed at heights of 2.05 and 3.25 m above the ground. Photosynthetically active radiation (PAR) was measured using a quantum sensor (model LI-190SB, Li-Cor Inc, USA). Solar radiation and net radiation (R_n) were measured by a pyranometer (model CM11, Kipp & Zonen, Delft, The Netherlands) and a net radiometer (model CNR-1, Kipp & Zonen, Delft, The Netherlands), respectively. Two soil heat flux plates were buried in the depth of 2 cm, one between rows and another between plants. Soil temperature was measured at 0, 5, 10, 30 and 50 cm depths. Soil water content (SWC) at the depths of 20 cm and 30 cm was measured with time domain reflectometers (TDR) (model CS616, Campbell Sci. Inc., USA). Rainfall was measured with a rain gauge (model 52203, Rm Young MI, USA). All meteorological data were recorded with a

data logger (model CR23x, Campbell Sci. Inc., USA) and were stored at intervals of 30 min.

Biomass, leaf area index (LAI) and plant height were measured every 5 days during the growing season of winter wheat. There were three sampling plots (replications) for each measurement. Twenty plants were sampled continuously for each plot and the plots were selected randomly. Leaf area was measured with Leaf area instrument (model Li-3100, Campbell Sci. Inc., USA). In this study, the main growing season began when the cropland turned from the carbon source to the sink (5-day moving mean CO₂ flux from positive to negative), and it ended when shifted reversely.

Flux data quality control

CO₂ and latent heat fluxes were calculated as follows:

$$F_c = \rho(\overline{w'c'}) \quad (1)$$

$$\lambda E = \lambda \rho(\overline{w'q'}) \quad (2)$$

where ρ is air density, w' the vertical wind velocity, c' CO₂ concentration, λ the latent heat of vaporization, E water vapor flux and q the specific humidity. Overbars indicate an averaging operation and primes denote deviations from the mean.

Raw data were conducted by two dimension coordinate rotations [31] and Webb-Pearman-Leuning (WPL) correction [32] to obtain 30-min mean flux data. CO₂ and water vapor fluxes could be affected by rain and dew. The abnormal data were eliminated following the method used by Falge et al. [33]. In the daytime, data gaps were 29%, 8%, 10% and 16% in the growing seasons of winter wheat in 2003, 2004, 2005 and 2006, respectively. Gap filled data were not used in this paper.

Light response of NEE

In most ecosystems, the relationship between daytime NEE and PAR can be expressed by a rectangular hyperbolic function [33,34]:

$$NEE = -\frac{\alpha P_{\max} PAR}{P_{\max} + \alpha PAR} + R_d \quad (3)$$

where α is the initial slope of the light response curve (initial light use efficiency), P_{\max} the maximum photosynthetic capacity, R_d the daytime ecosystem respiration rate under dark conditions. The model (Eq. (3)) was fitted by the software "Origin 7.0" (Microcal Software Inc.). In this study, negative NEE means net CO₂ uptake by the cropland and positive NEE indicates net CO₂ emission from the cropland.

To study the environmental factors influencing daytime NEE besides PAR, NEE was computed using Eq. (3) and the residual (NEE_r) was obtained as measured NEE minus simulated NEE. Stepwise multiple linear regression models were used to estimate the integrative influences of biophysical factors on NEE_r. Statistical analyses were performed using the software "SPSS 13.0" (SPSS Inc.). According to the method used by Carrara et al. [17], Powell et al. [18] and Teklemariam et al. [7], air temperature (T_a), vapor pressure deficit (VPD), soil water content (SWC), leaf area index (LAI) and canopy conductance (g_c) were divided into many classes and mean NEE_r was obtained for each class to show the trends in NEE_r versus variables.

To investigate seasonal patterns of light response parameters, a rectangular hyperbola (Eq. (3)) was used to describe the light response of NEE every five days and a time series of α , P_{\max} and R_d were obtained. Meanwhile, the biophysical variables in the daytime with the 5-day interval were averaged. Stepwise multiple linear regression analyses were applied to distinguish the key drivers for α , P_{\max} and R_d . The relationships among light response parameters were also investigated at the 5-day scale.

Light response parameters varied among years. Standard errors (e_1 and e_2) were calculated for sunny and cloudy sky conditions and total standard error (e) was obtained for both sky conditions using the equation as follows:

$$e = \frac{e_1 + e_2}{\sqrt{2}} \quad (4)$$

The difference between sunny and cloudy sky conditions would be pronounced if it was larger than the total standard error for two sky conditions.

Canopy conductance

According to Monteith and Unsworth [35], canopy conductance (g_c) was calculated as follows:

$$\frac{1}{g_c} = \frac{1}{g_a} \left[\frac{\Delta(R_n - G) + \rho C_p g_a VPD}{\lambda E \gamma} - \frac{\Delta}{\gamma} - 1 \right] \quad (5)$$

where λE is the latent heat flux (W m^{-2}), R_n net radiation (W m^{-2}), G soil heat flux (W m^{-2}), Δ the slope of saturation vapor pressure to the air temperature curve (kPa K^{-1}), ρ air density (mol m^{-3}), C_p the specific heat capacity of air ($\text{J mol}^{-1} \text{K}^{-1}$), VPD vapor pressure deficit (kPa), γ the psychrometric constant (kPa K^{-1}), g_c canopy conductance (m s^{-1}), and g_a aerodynamic conductance (m s^{-1}) which can be given as follows [36]:

$$\frac{1}{g_a} = r_a = \frac{\left(\ln \frac{z-d}{z_0} \right)^2}{k^2 u} \quad (6)$$

where r_a is aerodynamic resistance (s m^{-1}), z the height where wind velocity measured (m), d zero-plane displacement height (m), z_0 roughness length (m), k the von Karman constant (0.41) and u wind velocity (m s^{-1}). z_0 and d can be calculated as [37,38]:

$$z_0 = 0.13h \quad (7)$$

$$d = 0.75h \quad (8)$$

where h is the crop height (m).

Defining sunny and cloudy sky conditions

The clearness index (k_t) is used to describe sky conditions and the degree of impact of cloudiness on the solar radiation received at the Earth's surface [22]. It can be given by [39]:

$$k_t = \frac{S}{S_e} \quad (9)$$

$$S_e = S_{sc} [1 + 0.033 \cos(360t_d/365)] \sin \beta \quad (10)$$

$$\sin \beta = \sin \phi \sin \delta + \cos \phi \cos \delta \cos \omega \quad (11)$$

where S is global solar radiation (W m^{-2}), S_e the extraterrestrial irradiance at a plane parallel to the earth surface (W m^{-2}), S_{sc} the solar constant (1370 W m^{-2}), t_d the day of year, β the solar elevation angle, ϕ the local latitude, δ the declination of the sun, and ω hour angle. The sky conditions were classified at a half-day scale because the days without clouds for the whole daytime were rare [39]. In this study, sunny skies were simply identified when the half-day mean k_t was larger than a threshold in the morning and afternoon, respectively. 1.2 times of two-month running average k_t was used as the threshold so that the number of obtained sunny half-days was close to the mean value observed in recent decades. Clearness index were plotted against solar elevation angles and fitted by cubic polynomials in the sunny mornings and afternoons, respectively (Fig. 1). The data falling away from the major patterns were excluded [39]. Different from the studies in the forests [22,39], k_t observed in the wheat field was lower in the afternoon than in the morning (Fig. 1a). Air pollution may reduce the atmospheric transparency, resulting in a small incident solar radiation at the land surface. The reduction was more evident in the afternoon than in the morning (Fig. 1b).

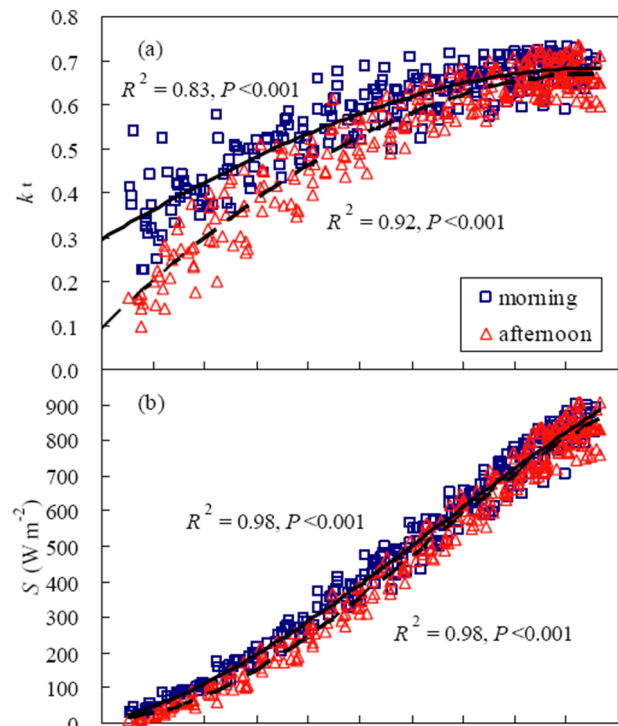


Figure 1. Scatter plots and regressions between (a) the clearness index (k_t) and the sine of solar elevation angles ($\sin \beta$), and (b) global solar radiation (S) and $\sin \beta$ for a winter wheat field in April-May 2003. The data were fitted by cubic polynomials in the morning (solid line) and afternoon (dashed line), respectively.

doi:10.1371/journal.pone.0089469.g001

Results

NEE Light response and influencing factors

The relationship between daytime NEE and PAR in a winter wheat field is shown in Figure 2. Light response curves in April and May were similar but both of them differed from those in March. From 2003 to 2006, P_{\max} was $46.6 \pm 4.0 \mu\text{mol CO}_2 \text{ m}^{-2} \text{ s}^{-1}$, α $0.059 \pm 0.006 \mu\text{mol } \mu\text{mol}^{-1}$ and R_d $5.3 \pm 0.3 \mu\text{mol CO}_2 \text{ m}^{-2} \text{ s}^{-1}$ in April–May, two or three times as high as those in March (Table 1). However, the inter-annual coefficients of variation (CV) for α , P_{\max} and R_d were great in March due to large variations of LAI, daytime mean T_a , VPD and SWC among years. The variations in VPD and SWC resulted from significant changes in precipitation in March among years (Tables 1 and 2). In March 2005, α was so small and P_{\max} was so large that the light response curves were actually close to a line (Table 1 and Fig. 2).

Table 3 indicates that NEE_r declined with the increases in LAI, g_c , T_a and SWC ($P < 0.001$) but increased with the increase in VPD ($P < 0.001$). Positive/negative NEE_r means measured NEE was higher/lower than simulated NEE; or measured CO_2 uptake was lower/higher than simulated CO_2 uptake. The impacts of biophysical factors on NEE_r varied in different months. Factors influencing NEE_r were sorted as LAI, SWC, g_c , T_a and VPD in March; g_c , LAI, VPD and T_a in April; and LAI, g_c , VPD and T_a in May. The effects of SWC on NEE_r were significant in March but insignificant in April and May (Table 3).

Shifted trends in NEE_r versus variables illustrated the limit in linear regression analysis (Fig. 3). With the increase in T_a and VPD, NEE_r turned to increase significantly ($P < 0.001$) when T_a was more than 25°C or VPD more than $1.1\text{--}1.3 \text{ kPa}$. With an increase in g_c , the NEE_r decline disappeared, or even turned into an increase ($P < 0.01$) when g_c exceed 26 mm s^{-1} in April or 14 mm s^{-1} in March and May (Fig. 3 and Table 4). No reverse trends were found for NEE_r versus LAI and SWC.

Light response parameters: seasonal variation and influencing factors

Light response parameters varied seasonally, with peaks in April or May ranged from 64.2 to $86.1 \mu\text{mol CO}_2 \text{ m}^{-2} \text{ s}^{-1}$ for P_{\max} , from 0.070 to $0.087 \mu\text{mol } \mu\text{mol}^{-1}$ for α and from 6.5 to $8.5 \mu\text{mol CO}_2 \text{ m}^{-2} \text{ s}^{-1}$ for R_d during the year 2003–2006 (Fig. 4). The seasonal patterns of P_{\max} were similar with LAI but different from T_a and VPD which have an increasing tendency from March to May. Compared with other years, P_{\max} peaked earlier in 2004 when LAI reached the maximum in mid-April due to fast warming in spring (Fig. 4).

Figure 5 shows the scattered points of biophysical factors (LAI, g_c , T_a , VPD and SWC) versus NEE light response parameters (α , P_{\max} and R_d) at 5-day scale during the main growing season of winter wheat. Stepwise multiple linear regression models were used to assess their relationships (Table 5). P_{\max} increased with the increase in LAI, g_c and T_a ($P < 0.001$) but reduced with the increase in VPD ($P < 0.001$). The factors influencing P_{\max} were sorted as LAI, g_c , T_a and VPD. α was proportional to $\ln(\text{LAI})$, g_c , T_a and VPD ($P < 0.001$). The impacts of LAI, g_c and T_a on α were larger than that of VPD. R_d was proportional to T_a ($P < 0.001$). It was better to express the relationship between R_d and T_a using exponential equation instead of linear equation. However, the influences of SWC on all light response parameters were insignificant (Table 5).

During the growing season of winter wheat, α increased linearly with an increase in R_d ($P < 0.001$) (Fig. 6). α and R_d enhanced firstly and then declined with the increase in P_{\max} . The maximum α and R_d appeared when P_{\max} was around $50 \mu\text{mol CO}_2 \text{ m}^{-2} \text{ s}^{-1}$. Their relationships could be expressed by quadratic polynomials ($P < 0.001$) (Fig. 6).

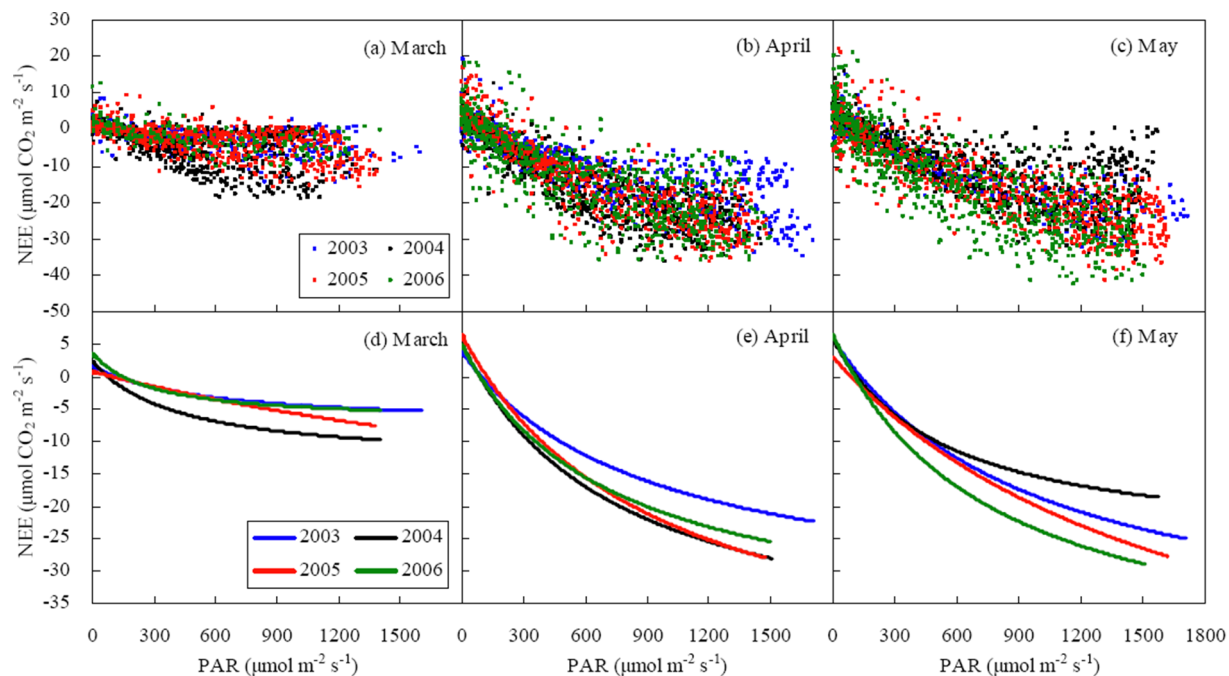


Figure 2. Response of net ecosystem CO_2 exchange (NEE) to photosynthetically active radiation (PAR) in a winter wheat field. a–c: NEE obtained by eddy covariance technique; d–f: light response curves fitted monthly using the rectangular hyperbolic function (Eq. (3)). The values of light response parameters were shown in Table 1. doi:10.1371/journal.pone.0089469.g002

Table 1. Monthly NEE light response parameters (P_{\max} , α and R_d) derived from Eq. (3) for a winter wheat field.

Month	Year	P_{\max} ($\mu\text{mol CO}_2 \text{ m}^{-2} \text{ s}^{-1}$)	α ($\mu\text{mol } \mu\text{mol}^{-1}$)	R_d ($\mu\text{mol CO}_2 \text{ m}^{-2} \text{ s}^{-1}$)	r^2	n
March	2003	9.2	0.017	1.6	0.388***	497
	2004	15.8	0.037	2.4	0.396***	681
	2005	29.9	0.008	0.8	0.360***	701
	2006	10.6	0.036	3.5	0.431***	179
April	2003	40.1	0.044	3.8	0.736***	695
	2004	49.7	0.067	5.2	0.836***	746
	2005	56.4	0.060	6.4	0.806***	719
	2006	44.8	0.063	5.0	0.629***	692
May	2003	48.7	0.050	5.9	0.876***	402
	2004	32.8	0.061	5.9	0.619***	779
	2005	64.5	0.036	3.1	0.723***	743
	2006	53.4	0.070	6.5	0.715***	754

P_{\max} : maximum photosynthetic capacity;

α : initial light use efficiency;

R_d : daytime ecosystem respiration under dark conditions.

Significance of the regression was "****" for $P < 0.001$.

doi:10.1371/journal.pone.0089469.t001

NEE Light response and NEE– g_c relationships under various sky conditions

Light response curves of NEE were determined under sunny and cloudy sky conditions, respectively (Fig. 7 and Table 6). The analyses were only conducted during the period with large LAI ($0.8\text{LAI}_{\max} < \text{LAI} < \text{LAI}_{\max}$) to limit the influences of crop growth on NEE light response. Compared with sunny sky conditions, P_{\max} under cloudy conditions was 19%, 12% and 27% higher in 2003, 2004 and 2006 but 14% lower in 2005; α under cloudy skies was 24% and 64% larger in 2003 and 2005, but 5% and 10% less in

2004 and 2006 (Table 6). On average, P_{\max} , α and R_d under cloudy sky conditions were 9%, 11% and 2% higher than those under sunny sky conditions, respectively. However, owing to large variation in α , P_{\max} and R_d among years, their differences between two sky conditions were smaller than their total standard errors calculated by Eq. (4) (Table 7), indicating unremarkable differences in light response parameters between sunny and cloudy sky conditions.

NEE Light response in cloudy days differed from that in sunny days. The differences between two light response curves were significant in 2003 and 2005 but insignificant in 2004 and 2006. Cloudy and sunny light response curves were so close in 2004 and 2006 that their differences were within the confidence intervals due to scattered points of NEE versus PAR (Fig. 7). At the same PAR, simulated net CO_2 uptake was 33%, 13%, 23% and 8% (averaged 18%) higher under cloudy sky conditions than under sunny sky conditions in 2003, 2004, 2005 and 2006, respectively. The difference between two sky conditions was more than their standard errors (Table 7), suggesting that net CO_2 uptake under cloudy sky conditions was significantly higher than that under sunny sky conditions.

As mentioned above, LAI and g_c were key factors affecting NEE. After neglecting the effects of LAI on NEE during the period with large LAI, the NEE– g_c relationships were investigated in several radiation classes (Fig. 8). The correlations between NEE and g_c were described by logarithmic equations under strong, moderate and weak radiation, respectively ($P < 0.001$). With the increase in $\ln(g_c)$, net CO_2 uptake enhanced more quickly under strong radiation than under low radiation. At the same g_c , net CO_2 uptake was higher in cloudy days than in sunny days. Nevertheless, the differences between two regression lines were insignificant for all PAR classes because they were within the wide confidence intervals owing to scattered points of NEE versus $\ln(g_c)$ (Fig. 8).

Table 2. Monthly biophysical variables in the winter wheat field from March to May in the year 2003–2006.

Month	Year	T_a ($^{\circ}\text{C}$)	VPD (kPa)	SWC ($\text{m}^3 \text{ m}^{-3}$)	Prec (mm)	LAI
March	2003	8.7	0.57	0.184	42.5	0.61
	2004	10.5	0.69	0.136	55.7	1.47
	2005	7.9	0.65	0.100	0.1	1.07
	2006	10.4	0.81	0.106	0.2	0.86
April	2003	15.3	0.73	0.186	160.3	3.20
	2004	17.1	0.88	0.141	52.4	5.69
	2005	17.2	0.96	0.139	27.5	4.49
	2006	15.7	0.79	0.124	19.7	3.81
May	2003	21.9	0.99	0.160	12.4	2.99
	2004	21.1	1.10	0.134	46.8	3.44
	2005	21.1	1.07	0.145	37.0	4.61
	2006	20.9	0.96	0.138	62.4	4.95

T_a : daytime mean air temperature;

VPD: daytime mean vapor pressure deficit;

SWC: daytime mean soil water content at a depth of 20 cm;

Prec: total precipitation;

LAI: mean leaf area index.

doi:10.1371/journal.pone.0089469.t002

Table 3. Influences of biophysical factors (T_a , VPD, SWC, g_c and LAI) on NEE residual in a winter wheat field from March to May in the year 2003–2006, estimated by the stepwise multiple linear regression models.

Month	Independent variables	F	r^2	Model
March	LAI	644.33***	0.289	$NEE_r = -2.854LAI + 2.813$
	LAI, SWC	382.77***	0.326	$NEE_r = -2.918LAI - 17.883SWC + 5.257$
	LAI, SWC, g_c	284.79***	0.350	$NEE_r = -2.732LAI - 16.507SWC - 0.126g_c + 5.498$
	LAI, SWC, g_c , T_a	215.08***	0.352	$NEE_r = -2.611LAI - 15.341SWC - 0.127g_c - 0.029T_a + 5.496$
	LAI, SWC, g_c , T_a , VPD	182.50***	0.366	$NEE_r = -2.461LAI - 10.812SWC - 0.112g_c - 0.149T_a + 1.883VPD + 4.499$
April	g_c	386.84***	0.125	$NEE_r = -0.289g_c + 2.855$
	g_c , LAI	315.42***	0.188	$NEE_r = -0.274g_c - 1.004LAI + 7.054$
	g_c , LAI, VPD	267.37***	0.228	$NEE_r = -0.247g_c - 1.130LAI + 2.214VPD + 5.329$
	g_c , LAI, VPD, T_a	211.68***	0.238	$NEE_r = -0.254g_c - 0.971LAI + 3.388VPD - 0.155T_a + 6.275$
May	LAI	570.78***	0.180	$NEE_r = -1.989LAI + 8.392$
	LAI, g_c	403.46***	0.237	$NEE_r = -1.738LAI - 0.268g_c + 9.709$
	LAI, g_c , VPD	277.50***	0.243	$NEE_r = -1.670LAI - 0.264g_c + 0.752VPD + 8.539$
	LAI, g_c , VPD, T_a	214.56***	0.249	$NEE_r = -1.777LAI - 0.264g_c + 1.788VPD - 0.188T_a + 11.925$

NEE_r: NEE residual, $\mu\text{mol CO}_2 \text{ m}^{-2} \text{ s}^{-1}$ (the dependent variable);

g_c : canopy conductance, mm s^{-1} .

The meanings and units of T_a , VPD, SWC and LAI were the same as Table 2.

Significance of the regression was "****" for $P < 0.001$.

doi:10.1371/journal.pone.0089469.t003

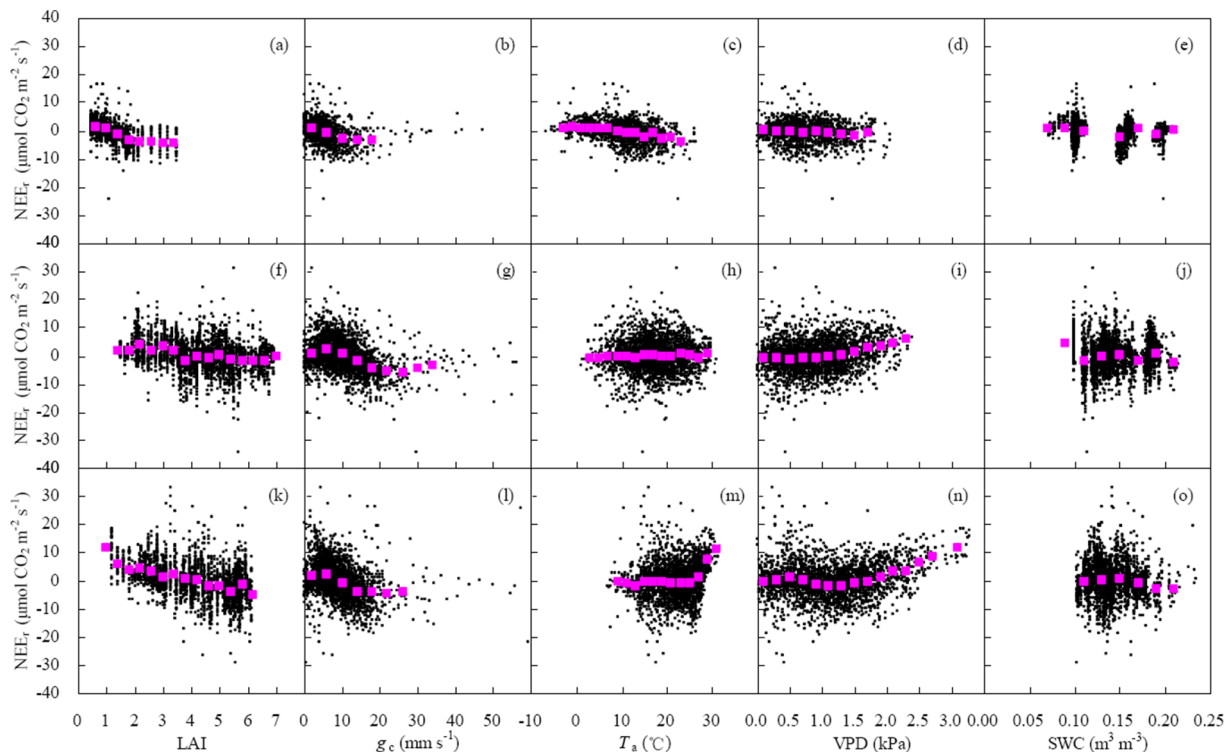


Figure 3. Effects of biophysical factors on NEE residual (NEE_r) in a winter wheat field in March (a–e), April (f–j) and May (k–o). NEE residual was measured NEE minus simulated NEE. The simulated NEE was obtained by Eq. (3). Biophysical factors include canopy conductance (g_c), Leaf area index (LAI), daytime air temperature (T_a), vapor pressure deficit (VPD) and soil water content at the depth of 20 cm (SWC).
doi:10.1371/journal.pone.0089469.g003

Table 4. Correlation coefficients between NEE residual and influencing variables when the variables were less or more than the thresholds.

Variable	Month	Threshold	Correlation coefficient	
			Variable< Threshold	Variable> Threshold
T_a	May	25°C	-0.006	0.478***
VPD	April	1.1 kPa	0.012	0.268***
	May	1.3 kPa	-0.133	0.481***
g_c	March	14 mm s ⁻¹	-0.353***	0.402**
	April	26 mm s ⁻¹	-0.375***	0.029
	May	14 mm s ⁻¹	-0.283***	0.076

Significances of the regression were “**” for $P < 0.01$ and “***” for $P < 0.001$.
doi:10.1371/journal.pone.0089469.t004

Discussion

Factors influencing NEE light response

In boreal and temperate forests, NEE_r generally declines with increasing T_a and VPD. These trends turn to rise when T_a exceeds 20–25°C [7,17] and VPD exceeds 1.1–1.3 kPa [7,18]. In this study, similar phenomena were observed beyond the same thresholds in a temperate cropland (Fig. 3 and Table 4). However, in the tropical forest, NEE_r always increases with the increase in T_a and VPD without reverse trends [40] (Loescher et al., 2003). It may be ascribed to high air temperature and humidity with a narrow range in the tropic region.

Net CO₂ uptake decreased with the increase in T_a and VPD (Fig. 3), indicating that temperature and water stress occurred. Under high temperature ($T_a > 25^\circ\text{C}$), photosynthesis was prohibited and soil and plant respirations were great, resulting in a lower net CO₂ uptake than the one simulated by Eq. (3). On the other hand, VPD controls photosynthetic rate through influencing stomatal closure. Under higher VPD, stomatal opening is smaller,

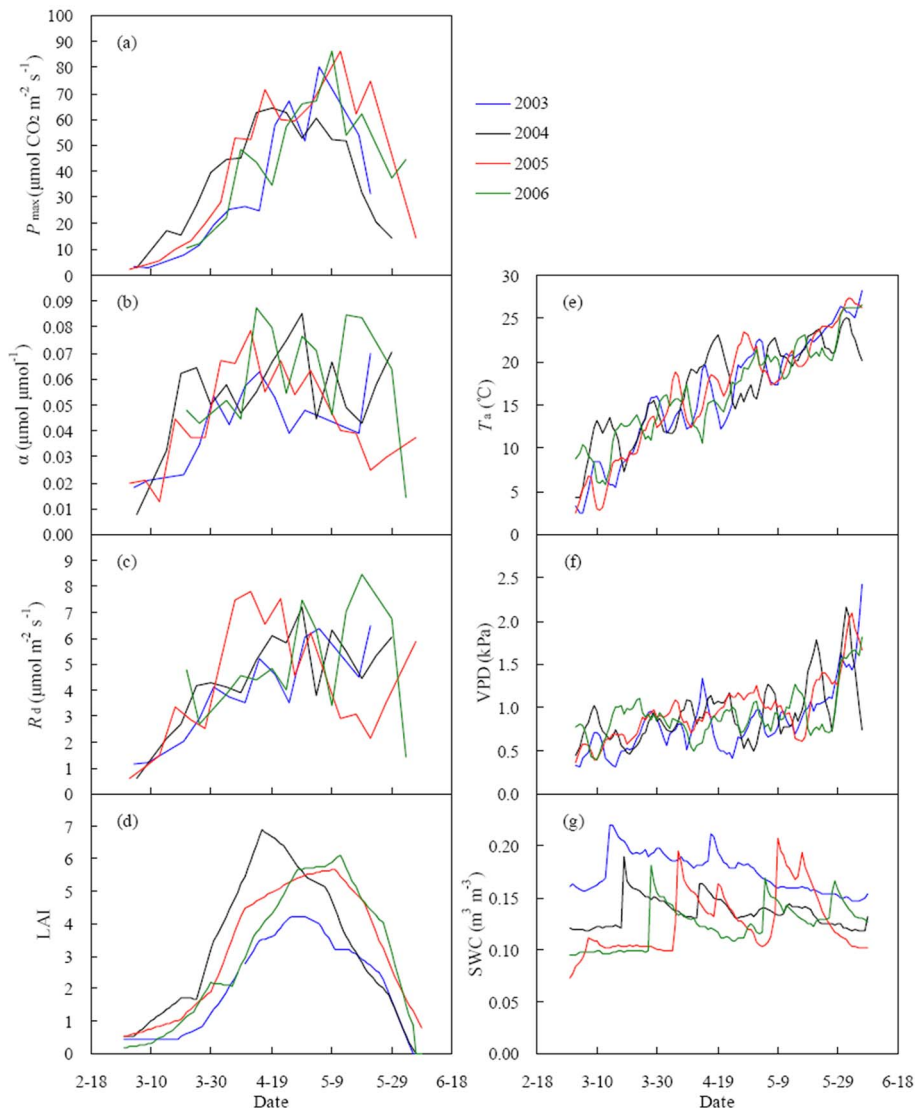


Figure 4. Seasonal variation of initial light use efficiency (α), maximum photosynthetic capacity (P_{max}), daytime ecosystem respiration under dark conditions (R_d), air temperature (T_a), vapor pressure deficit (VPD) and leaf area index (LAI) in a winter wheat field during the main growing season. α , P_{max} and R_d were obtained at 5-day intervals using a regression model (Eq. (3)).
doi:10.1371/journal.pone.0089469.g004

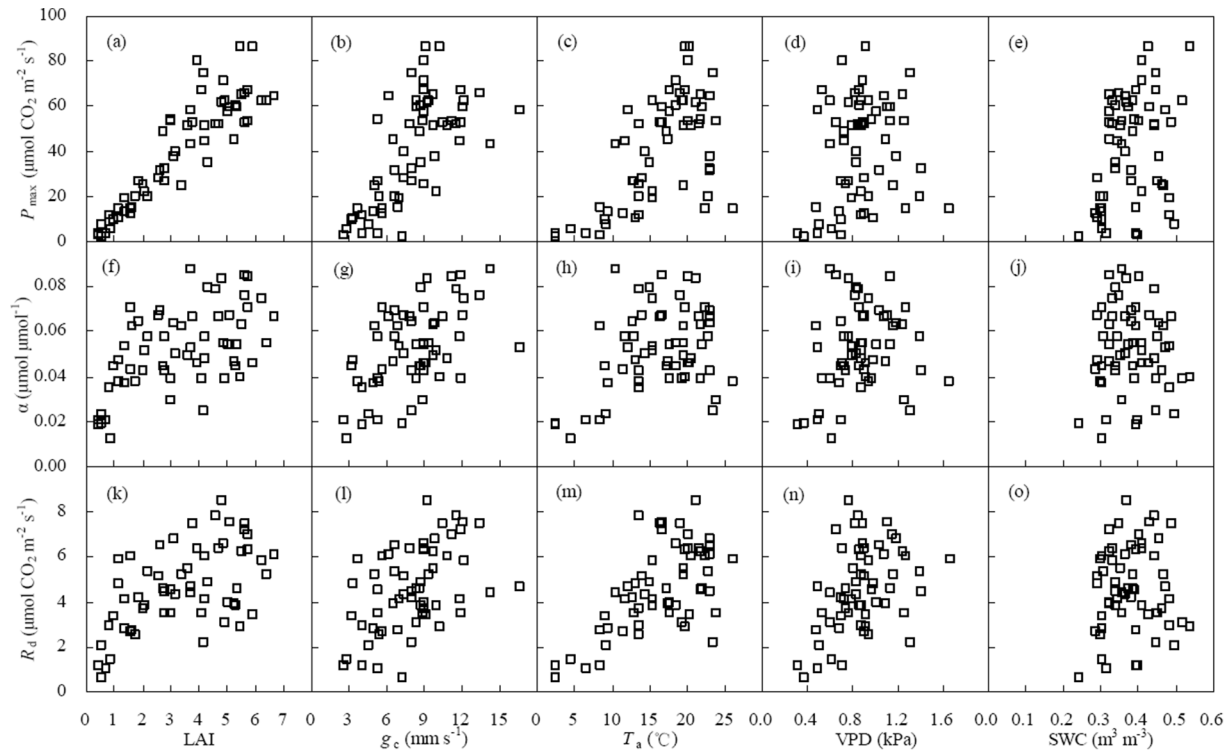


Figure 5. Effects of biophysical factors (g_c , LAI, T_a , VPD and SWC) on light response parameters (α , P_{\max} and R_d) at 5-day intervals during the main growing season of winter wheat. The meanings of abbreviates were the same as those in Figures 3 and 4. doi:10.1371/journal.pone.0089469.g005

leading to the decrease of photosynthetic rate [41]. Moreover, the decline of photosynthetic rate was likely due to low leaf water potential caused by high transpiration rates [42]. Ecosystem respiration is large under higher VPD because of high air and soil temperatures [41]. Hence, net carbon uptake by the cropland dropped. In this study, lower VPD threshold in April than in May (Table 4) implied that wheat plants were more sensitive to the drought at the fast growing stage than at the senescence stage.

Around the critical value, the reverse trends in NEE_r versus g_c (Fig. 3 and Table 4) suggested a shift from stomatal limitation to non-stomatal limitation on daytime net CO_2 exchange. At dawn, dusk or in cloudy days, photosynthesis was inhibited by weak radiation even though g_c was large. Higher g_c threshold in April than in March and May (Table 4) indicated that net CO_2 uptake was more sensitive to stomatal behavior at the rapid growth stage than at the slow growth senescence stage. Therefore, NEE_r was

Table 5. Effects of biophysical drivers (LAI, g_c , T_a , VPD and SWC) on light response parameters (P_{\max} , α and R_d) at the 5-day scale estimated by the stepwise multiple linear regression models during the growing seasons of 2003–2006.

Dependent variables	Independent variables	F	r^2	Model
P_{\max}	LAI	267.65***	0.812	$P_{\max} = 11.8184LAI + 1.0615$
	LAI, g_c	145.05***	0.826	$P_{\max} = 10.3964LAI + 1.2911g_c - 4.6225$
	LAI, g_c , T_a	111.03***	0.847	$P_{\max} = 8.9964LAI + 1.6064g_c + 0.7171T_a - 14.4703$
	LAI, g_c , T_a , VPD	105.74***	0.878	$P_{\max} = 8.1875LAI + 1.0694g_c + 1.9627T_a - 26.0434VPD - 4.6112$
α	T_a	11.40**	0.155	$\alpha = 0.0015T_a + 0.0273$
	T_a , g_c	8.62***	0.220	$\alpha = 0.0013T_a + 0.0019g_c + 0.0151$
	T_a , g_c , VPD	8.19***	0.291	$\alpha = -0.0002T_a + 0.0030g_c + 0.0354VPD - 0.0001$
	g_c , VPD	12.43***	0.290	$\alpha = 0.0029g_c + 0.0320VPD + 0.0005$
α	$\ln(LAI)$	14.07***	0.185	$\alpha = 0.029\ln(LAI) + 0.040$
	$\ln(LAI)$, VPD	11.71***	0.277	$\alpha = 0.026\ln(LAI) + 0.023VPD + 0.021$
R_d	T_a	31.98***	0.340	$R_d = 0.221T_a + 0.897$
$\ln(R_d)$	T_a	32.35***	0.343	$\ln(R_d) = 0.027T_a + 0.145$

The meanings and units of biophysical factors and light response parameters were the same as Tables 1, 2 and 3. Significances of the regression were *** for $P < 0.01$ and **** for $P < 0.001$. doi:10.1371/journal.pone.0089469.t005

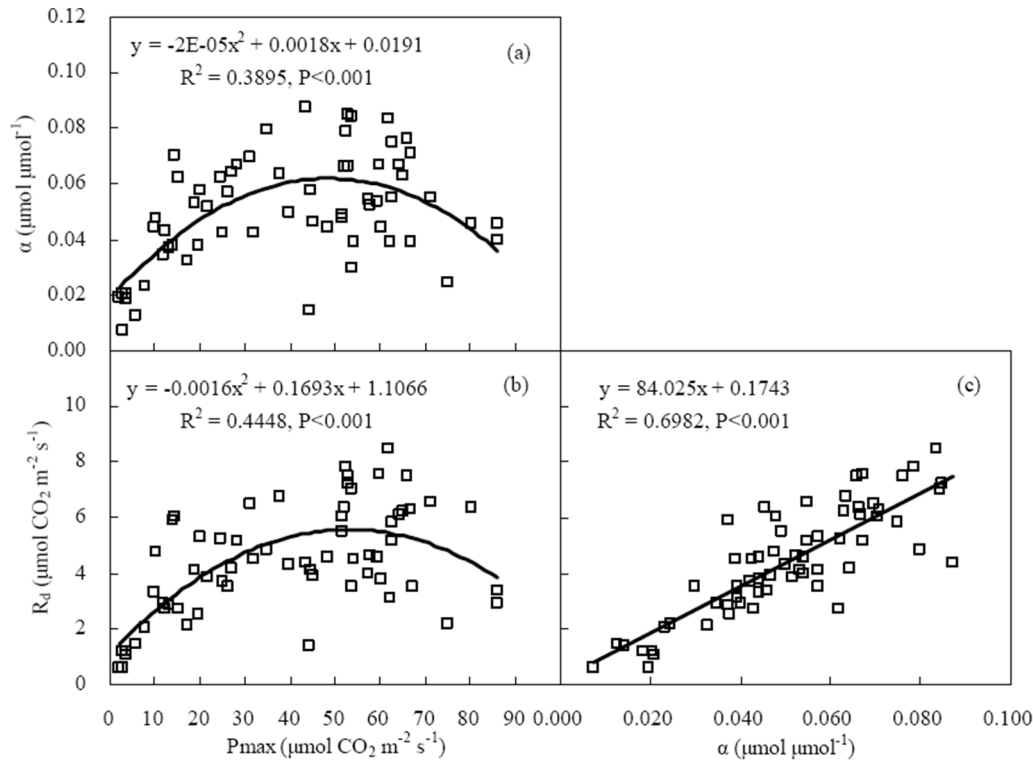


Figure 6. Relationships among initial light use efficiency (α), maximum photosynthetic capacity (P_{\max}), and daytime ecosystem respiration under dark conditions (R_d) at 5-day intervals during the main growing season of winter wheat.
doi:10.1371/journal.pone.0089469.g006

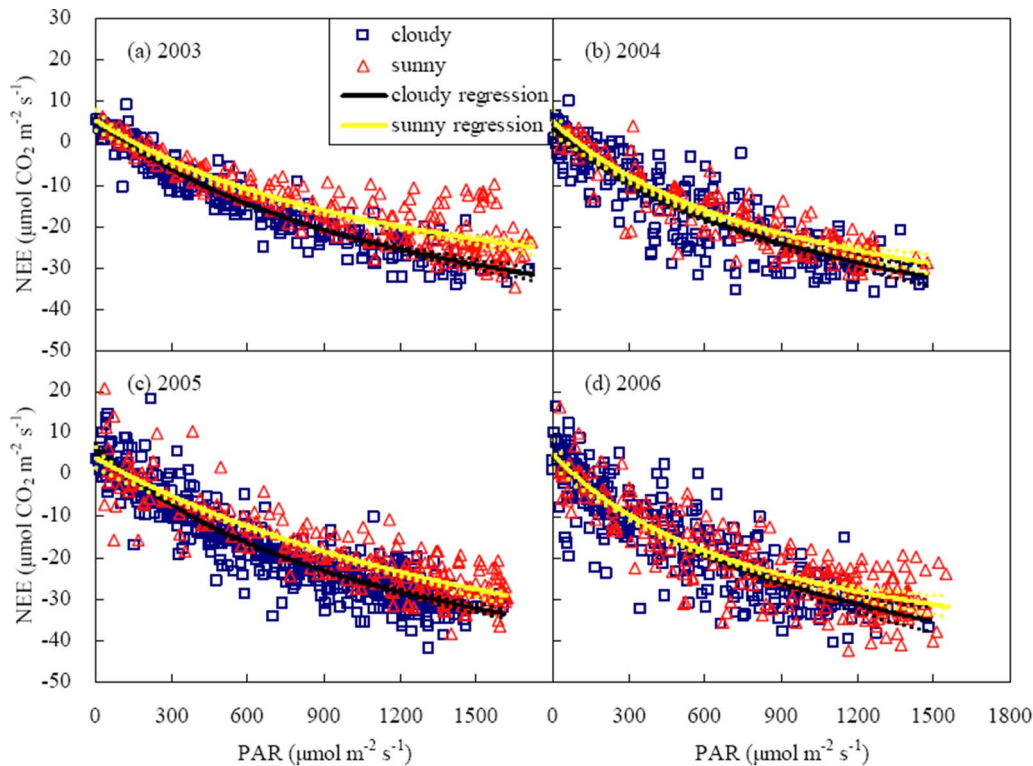


Figure 7. Response of NEE to PAR under sunny and cloudy sky conditions in a winter wheat field during the period of large leaf area index ($0.8LAI_{\max} < LAI < LAI_{\max}$). Light response curves (solid curves) were fitted using the rectangular hyperbolic function (Eq. (3)). The values of light response parameters were shown in Table 3. Between the upper and lower dotted curves were 95% confidence intervals.
doi:10.1371/journal.pone.0089469.g007

Table 6. NEE light response parameters (P_{\max} , α and R_d) derived from Eq.(3) under sunny and cloudy sky conditions in a winter wheat field during the period of large leaf area index ($0.8LAI_{\max} < LAI < LAI_{\max}$).

Year	Sky condition	P_{\max} ($\mu\text{mol CO}_2 \text{ m}^{-2} \text{ s}^{-1}$)	α ($\mu\text{mol } \mu\text{mol}^{-1}$)	R_d ($\mu\text{mol CO}_2 \text{ m}^{-2} \text{ s}^{-1}$)	r^2	n
2003	Sunny	56.0	0.039	5.3	0.812***	226
	Cloudy	66.8	0.049	5.4	0.920***	302
2004	Sunny	57.5	0.056	5.0	0.839***	143
	Cloudy	64.7	0.054	3.2	0.790***	261
2005	Sunny	83.0	0.034	3.8	0.799***	231
	Cloudy	71.2	0.056	6.1	0.881***	567
2006	Sunny	57.2	0.066	4.8	0.747***	231
	Cloudy	72.8	0.059	4.5	0.766***	325

Significance of the regression was "****" for $P < 0.001$.
doi:10.1371/journal.pone.0089469.t006

mainly controlled by g_c instead of LAI in April. However, when g_c was limited in colder March or drier May, LAI became the most important factor affecting NEE_s in these months.

The significant impacts of SWC on NEE_s in March (Table 3) may be ascribed to large variation in soil moisture before and after irrigation at the turning green stage of winter wheat (Fig. 4). Nevertheless, the sufficient irrigation concealed these effects in the following two months (Table 3).

Factors influencing light response parameters

Photosynthetic light response parameters were not constant but varied seasonally [9,11,19]. For wheat canopy, mean P_{\max} in April–May observed in this study ($49 \mu\text{mol CO}_2 \text{ m}^{-2} \text{ s}^{-1}$) was lower than the results ($62\text{--}67 \mu\text{mol CO}_2 \text{ m}^{-2} \text{ s}^{-1}$) obtained in a winter wheat field in central Germany [5] and a spring wheat field in Manitoba, Canada [43]. Mean α in April–May obtained in this study ($0.056 \mu\text{mol } \mu\text{mol}^{-1}$) was lower than the value ($0.063 \mu\text{mol } \mu\text{mol}^{-1}$) observed in a winter wheat field in central Germany [5], but higher than that ($0.036 \mu\text{mol } \mu\text{mol}^{-1}$) obtained in a spring wheat field in Manitoba, Canada [43]. The magnitudes of light response parameters varied among different studies might be attributed to the discrepancy in temperature, humidity, canopy structure or/and other factors.

P_{\max} had positive correlations with LAI [9,16,18,19], air temperature [17,18] and SWC [9,18] but negative correlation with VPD [9,44]. A similar phenomenon was found in this study (Fig. 5 and Table 5). Among all factors, LAI was regarded as a key factor controlling P_{\max} [9,16,18]. P_{\max} increased linearly [18] or nonlinearly [16,19] with increasing LAI. The nonlinear relationship was expected as the leaves shade each other in the ecosystem with higher vegetation density [16]. In the cropland, the linear correlation between P_{\max} and LAI (Fig. 5 and Table 5) illustrated a suitable density range for canopy light intercept.

LAI determines photosynthetic area while g_c controls the photosynthetic intensity. Owing to the strong link between g_c and photosynthetic rate, the influences of environmental factors (T_a , VPD and SWC) on photosynthesis may be ascribed to their effects on g_c [45]. Hence, factors influencing P_{\max} was sorted by LAI, g_c , T_a and VPD (Table 5). Our results in an irrigated wheat field differed from those obtained by Zhang et al. [9] who found that P_{\max} was only affected by LAI and VPD in a dry wheat field.

In this study, α was affected by LAI, T_a , g_c and VPD in an irrigated wheat field (Table 5), differing from the result reported by Zhang et al. [9] who found that α was only influenced by LAI in a dry wheat field. α represents weak light use efficiency by the plants. At dawn and dusk, the weak light is mainly composed of diffuse radiation. Under low LAI, less diffuse radiation was obtained by

Table 7. Comparisons of light response parameters and simulated NEE (NEE_s) under sunny and cloudy sky conditions.

Items	Sky conditions	Average	Standard error	Difference (Cloudy-Sunny)	Total Standard error	Ratio (Cloudy/Sunny)
P_{\max} ($\mu\text{mol CO}_2 \text{ m}^{-2} \text{ s}^{-1}$)	Sunny	63.42	6.53	5.45	5.95	1.09
	Cloudy	68.87	1.88			
α ($\mu\text{mol } \mu\text{mol}^{-1}$)	Sunny	0.0489	0.0074	0.0055	0.0068	1.11
	Cloudy	0.0544	0.0022			
R_d ($\mu\text{mol CO}_2 \text{ m}^{-2} \text{ s}^{-1}$)	Sunny	4.75	0.32	0.08	0.67	1.02
	Cloudy	4.83	0.62			
NEE_s ($\mu\text{mol CO}_2 \text{ m}^{-2} \text{ s}^{-1}$)	Sunny	-16.02	1.12	-2.90*	1.20	1.18
	Cloudy	-18.92	0.58			

For each year, NEE was calculated at the same PAR using Eq. (3) and the light response parameters in Table 6. The mean values were obtained for two sky conditions and total standard error was computed using Eq. (4).

The meanings of P_{\max} , α and R_d were the same as Tables 1.

Significance of the difference was "*" for $P < 0.05$ if the absolute difference between two sky conditions was greater than the total standard error.

doi:10.1371/journal.pone.0089469.t007

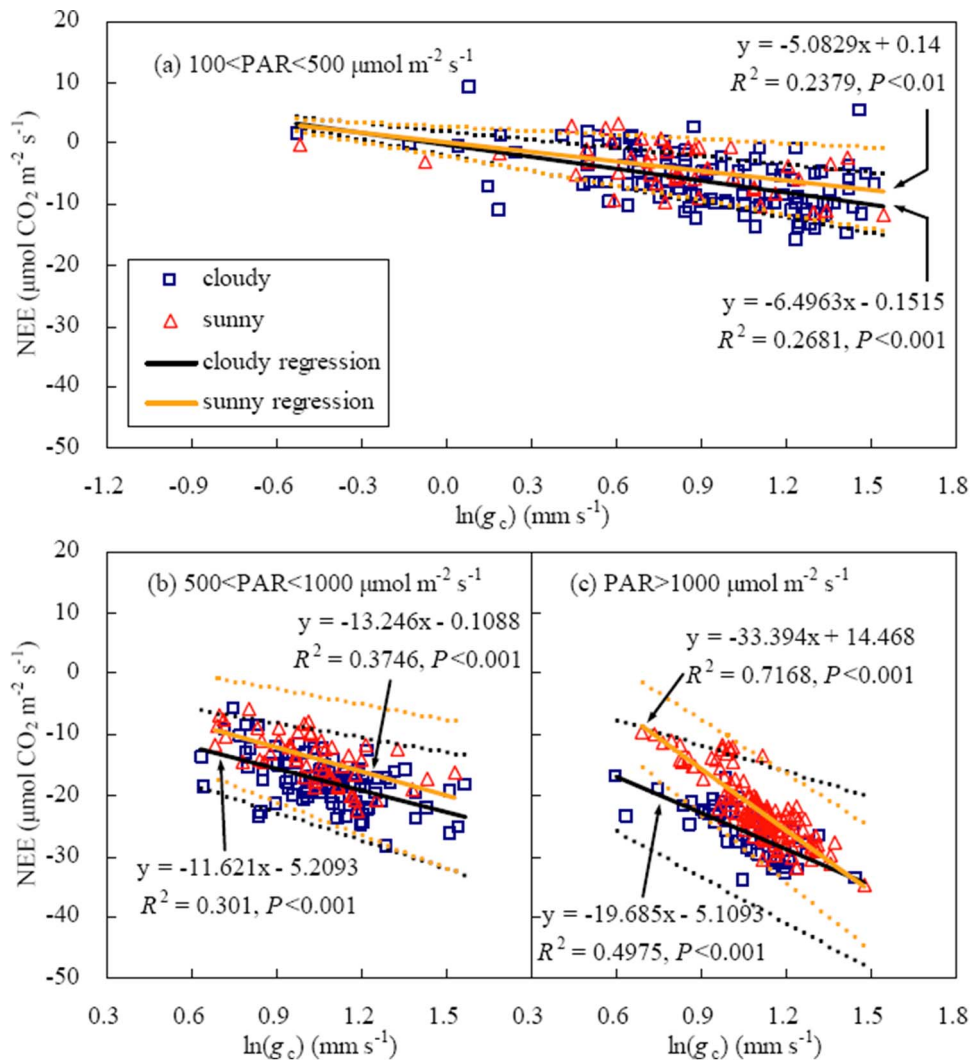


Figure 8. Linear relationship between NEE and logarithmic canopy conductance (g_c) under sunny and cloudy sky conditions (solid lines) in a winter wheat field during the period of large LAI ($0.8LAI_{max} < LAI < LAI_{max}$). Between the upper and lower dotted lines were 95% confidence intervals.

doi:10.1371/journal.pone.0089469.g008

the short canopy. When LAI enlarged, the canopy structure was beneficial to receiving scatter light from each direction. Less diffuse radiation was intercepted by the sparse canopy when LAI decreased with leaf senescence. Moreover, at dawn and dusk, low radiation led to small g_c . Under cold and moist conditions, α was more sensitive to T_a and g_c than to VPD.

Generally, the key factor influencing respiration was temperature (Table 5). It likely changed to moisture under dry conditions. For instance, Zhang et al. [9] obtained that R_d had positive correlations with LAI and soil moisture in a dry wheat field. In this study, R_d was correlated with T_a significantly but not related to VPD and SWC (Table 5 and Fig. 5) due to sufficient irrigation in the winter wheat field. Furthermore, the effect of LAI on R_d was unremarkable (Table 5 and Fig. 5) because R_d was composed of soil and plant respiration and only the later part was related to LAI [16].

After investigating the flux data observed in the grasslands and croplands over the world, Gilmanov et al. [19] pointed out that light response parameters were correlated with each other. Because P_{max} was proportional to LAI, α and R_d correlated to

P_{max} was the same as correlated to LAI (Table 5, Figs. 5 and 6). Positive correlation between α and R_d may result from a relatively stable critical PAR (PAR under zero NEE) of 110 ± 6 , 99 ± 6 , 102 ± 7 and $101 \pm 9 \mu\text{mol m}^{-2} \text{s}^{-1}$ in 2003, 2004, 2005 and 2006, respectively.

NEE Light response and NEE– g_c relations under various sky conditions

P_{max} in a wheat field was greater under cloudy skies than under sunny skies in most of years (Table 6), in agreement with the studies in the temperate forests [8,21,22]. Different from the temperate area, Zhang et al. [22] observed a reverse phenomenon in a subtropical forest: net CO_2 uptake under cloudy skies was less than that under sunny skies. It may be owing to much lower radiation intensity in cloudy days compared with sunny days in the subtropical forest. In the winter wheat field, differences of P_{max} and α between two sky conditions were insignificant (Table 6) due to large variations in P_{max} and α among years. The values of α in this study were consistent with those reported by Dengel and Grace [8] and Zhang et al. [22] for forests, but different from the

results observed by Hollinger et al. [10], Rocha et al. [21] and Suyker et al. [24] who obtained a larger α under cloudy conditions in the forests and an irrigated maize cropland.

In spite of no significant differences in light response parameters between sky conditions, simulated net CO₂ uptake under cloudy sky conditions was greater than that under sunny sky conditions at the same PAR (Fig. 7). A similar phenomenon was observed in the temperate forests [8,21] and the irrigated cropland [24]. More CO₂ uptake by the canopy under cloudy skies than that under sunny skies was owing to many reasons. Firstly, the proportion of diffuse radiation increases under cloudy sky conditions and more light can reach below leaves of the canopies [46]. Photosynthetic rates of shaded leaves are promoted by the delivery of diffuse radiation [47]. In addition, compared with shaded leaves, the phenomenon of saturating photosynthesis easily happens for sunlit leaves because shaded leaves often illuminate brightly [48]. Secondly, canopy conductance was usually higher under cloudy sky conditions than that under sunny sky conditions. Diffuse radiation enhances canopy stomatal conductance mainly due to the reduction in VPD and blue light enrichment within the canopy during cloudy and overcast weather [49,50–52]. Both low VPD

[53] and blue light [54,55] can stimulate stomatal opening and then enhance photosynthetic rate.

In this study, NEE– g_c relationships were expressed by logarithmic equations (Fig. 8), differing from the result obtained by Dengel and Grace [8] who pointed out that net CO₂ uptake enhanced linearly with the increase in g_c . Under strong radiation, net CO₂ uptake enhanced quickly with increasing g_c (Fig. 8), indicating that g_c was the main factor affecting NEE. Compared with cloudy days, net CO₂ uptake was more sensitive to the variation in g_c for higher temperature and VPD in sunny days.

Acknowledgments

We are particularly grateful to Prof. Xiaomin Sun, Assoc. Prof. Zhilin Zhu and Mr. Zhenmin Liu for their assistance with field measurements and instrumentation maintenance, and the editor and two anonymous reviewers for their constructive comments on the manuscript.

Author Contributions

Conceived and designed the experiments: XT JL QY. Performed the experiments: JL XT. Analyzed the data: JL XT. Contributed reagents/materials/analysis tools: QY JL ZL. Wrote the paper: XT JL.

References

- Farquhar GD, Caemmerer S, Berry A (1980) A biochemical model of photosynthetic CO₂ assimilation in leaves of C₃ species. *Planta* 149: 78–90.
- Harley PC, Thomas RB, Reynolds JF, Strain BR (1992) Modelling photosynthesis of cotton grown in elevated CO₂. *Plant Cell Environ* 15: 271–282.
- Hollinger DY, Kelliher FM, Schulze E-D, Bauer G, Arneth A, et al. (1998) Forest-atmosphere carbon dioxide exchange in eastern Siberia. *Agric For Meteorol* 90: 291–306.
- Flanagan LB, Wever LA, Carlson PJ (2002) Seasonal and interannual variation in carbon dioxide exchange and carbon balance in a Northern temperate grassland. *Global Change Biol* 8: 599–615.
- Anthoni PM, Knohl A, Rebmann C, Freibauer A, Mund M (2004) Forest and agricultural land-use-dependent CO₂ exchange in Thuringia, Germany. *Global Change Biol* 10: 2005–2019.
- Li J, Yu Q, Sun X, Tong X, Ren C, et al. (2006) Carbon dioxide exchange and the mechanism of environmental control in a farmland ecosystem in North China Plain. *Sci China Ser D* 49 (Suppl. II): 226–240.
- Teklemariam T, Staebler RM, Barr AG (2009) Eight years of carbon dioxide exchange above a mixed forest at Borden, Ontario. *Agric For Meteorol* 149: 2040–2053.
- Dengel S, Grace J (2010) Carbon dioxide exchange and canopy conductance of two coniferous forests under various sky conditions. *Oecologia* 164: 797–808.
- Zhang P, Chen SP, Zhang WL, Miao HX, Chen JQ, et al. (2012) Biophysical regulations of NEE light response in a steppe and a cropland in Inner Mongolia. *J Plant Ecol* 5(2): 238–248.
- Hollinger DY, Kelliher FM, Byers JN, Hunt JE, McSeveny TM, et al. (1994) Carbon dioxide exchange between an undisturbed old growth temperate forest and the atmosphere. *Ecology* 75: 134–150.
- Aubinet M, Chermanne B, Vandenhaute M, Longdoz B, Yernaux M, et al. (2001) Long term carbon dioxide exchange above a mixed forest in the Belgian Ardennes. *Agric For Meteorol* 108: 293–315.
- Gilmanov TG, Verma SB, Sims PL, Meyers TP, Bradford JA, et al. (2003) Gross primary production and light response parameters of four Southern Plains ecosystems estimated using long-term CO₂-flux tower measurements. *Global Biogeochem Cycles* 17(2): 1071, doi:10.1029/2002GB002023.
- Hirata R, Hirano T, Saigusa N, Fujinuma Y, Inukai K, et al. (2007) Seasonal and inter-annual variations in carbon dioxide exchange of a temperate larch forest. *Agric For Meteorol* 147: 110–124.
- Giasson M-A, Coursolle C, Margolis HA (2006) Ecosystem-level CO₂ fluxes from a boreal cutover in eastern Canada before and after scarification. *Agricultural and Forest Meteorology*, 140 23–40.
- Migliavacca M, Meroni M, Manca G, Matteucci G, Montagnani L, et al. (2009) Seasonal and interannual patterns of carbon and water fluxes of a poplar plantation under peculiar eco-climatic conditions. *Agricultural and Forest Meteorology*, 149: 1460–1476.
- Laurila T, Soegaard H, Lloyd C R, Aurela M, Tuovinen J-P, et al. (2001) Seasonal variations of net CO₂ exchange in European Arctic ecosystems. *Thero Appl Climatol* 70: 183–201.
- Carrara A, Janssens IA, Curiel Yuste J, Ceulemans R (2004) Seasonal changes in photosynthesis, respiration and NEE of a mixed temperate forest. *Agric For Meteorol* 126: 15–31.
- Powell TL, Bracho R, Li J, Dore S, Hinkle CR, et al. (2006) Environmental controls over net ecosystem carbon exchange of scrub oak in central Florida. *Agric For Meteorol* 141: 19–34.
- Gilmanov TG, Aires L, Barcza Z, Baron VS, Bellelli L, et al. (2010) Productivity, respiration, and light-response parameters of world grassland and agroecosystems derived from flux-tower measurements. *Rangeland Ecol Manage* 63: 16–39.
- Wild M (2009) Global dimming and brightening: a review. *J Geophys Res* 114:D00D16, doi:10.1029/2008JD011470.
- Rocha AV, Su HB, Vogel CS, Schmid HP, Curtis PS (2004) Photosynthetic and water use efficiency responses to diffuse radiation by an aspen-dominated northern hardwood forest. *Forest Sci* 50 (6): 793–801.
- Zhang M, Yu GR, Zhang LM, Sun XM, Wen XF, et al. (2010) Impact of cloudiness on net ecosystem exchange of carbon dioxide in different types of forest ecosystem in China. *Biogeosciences* 7: 711–722.
- Urban O, Klem K, Ač A, Havránková K, Holířová P, et al. (2012) Impact of clear and cloudy sky conditions distribution of photosynthetic CO₂ spruce canopy. *Funct Ecol* 26: 46–55.
- Suyker AE, Verma SB, Burba GG, Arkebauer TJ, Walters DT, et al. (2004) Growing season carbon dioxide exchange in irrigated and rainfed maize. *Agric For Meteorol* 124: 1–13.
- Béziat P, Ceschia E, Deduc G (2009) Carbon balance of a three crop succession over two cropland sites in South West France. *Agric For Meteorol* 149: 1628–1645.
- Wild M, Roesch A, Ammann C (2012) Global dimming and brightening – evidence and agricultural implications. *CAB Reviews* 7(003): 1–7.
- Mercado LM, Bellouin N, Sitch S, Boucher O, Huntingford C, Wild M, et al. (2009) Impact of changes in diffuse radiation on the global land carbon sink. *Nature* 458: 1014–1017.
- Wang F, He ZH, Ken Sayre K, Li SD, Si JS, et al. (2009) Wheat cropping systems and technologies in China. *Field Crop Res* 111: 181–188.
- NBSC, National Bureau of Statistics of China, 1998. *China Statistical Yearbook*. China Stat. Press, Beijing.
- Tong XJ, Li J, Zhang XS, Yu Q, Qin Z, et al. (2007) Mechanism and bio-environmental controls of ecosystem respiration in a cropland in the North China Plains. *New Zeal J Agr Res* 50 (5): 1347–1358.
- McMillen RT (1988) An eddy correlation technique with extended applicability to non-simple terrain. *Boundary Layer Meteorol* 43: 231–245.
- Webb EK, Pearman GI, Leuning R (1980) Correction of flux measurements for density effects due to heat and water vapor transfer. *Quart J R Meteorol Soc* 106: 85–100.
- Falge E, Baldocchi D, Olson R, Anthoni P, Aubinet M, et al. (2001) Gap filling strategies for defensible annual sums of net ecosystem exchange. *Agric For Meteorol* 107: 43–69.
- Ruimy A, Jarvis PG, Baldocchi DD, Saugier B (1995) CO₂ fluxes over plant canopies and solar radiation: A review. *Adv Ecol Res* 26: 1–68.
- Monteith JL, Unsworth MH (1990) *Principles of Environmental Physics*, second ed. Edward Arnold, London.
- Monteith JL (1965) Evaporation and environment, in *The state and Movement of Water in Living Organisms*, Sym. Soc. Exp. Biol., Vol XI X, 205–234, Company of Biologists, Cambridge, England.

37. Rutter AJ, Kershaw KA, Robins PC, Morton AJ (1971) A predictive model of rainfall interception in forests. I. Derivation of the model from observations in a plantation of Corsican pine. *Agric Meteorol* 9: 367–384.
38. Lhomme J-P (1991) The concept of canopy resistance: historical survey and comparison of different approaches. *Agric For Meteorol* 54: 227–240.
39. Gu L, Fuentes JD, Shugart HH, Staebler RM, Black TA (1999) Response of net ecosystem exchanges of carbon dioxide to changes in cloudiness: results from two North American deciduous forests. *J Geophys Res* 104 (D24): 31,421–31,434.
40. Loescher HW, Oberbauer SF, Gholz HL, Clark DB (2003) Environmental controls on net ecosystem-level carbon exchange and productivity in a Central American tropic wet forest. *Global Change Biol* 9: 396–412.
41. Anthoni PM, Law BE, Unsworth MH (1999) Carbon and water vapor exchange of an open-canopied ponderosa pine ecosystem. *Agric For Meteorol* 95: 151–168.
42. Hirasawa T, Hsiao TC (1999) Some characteristics of reduced leaf photosynthesis at midday in maize growing in the field. *Field Crop Res* 62: 53–62.
43. Glenn AJ, Amiro BD, Tenuta M, Stewart SE, Wagner-Riddle C (2010) Carbon dioxide exchange in a northern Prairie cropping system over three years. *Agric For Meteorol* 150: 908–918.
44. Dufranne D, Moureaux C, Vancutsem F, Bodson B, Aubinet M (2011) Comparison of carbon fluxes, growth and productivity of a winter wheat crop in three contrasting growing seasons. *Agr Ecosyst Environ* 141: 133–142.
45. Flexas J and Medrano H (2002) Drought-inhibition of photosynthesis in C3 Plants: Stomatal and Non-stomatal limitations revisited. *Ann Bot* 89: 183–189.
46. Jarvis PG, James GB, Landsberg JJ (1976) Coniferous forest. In: *Vegetation and the Atmosphere* (ed. Monteith J L), 171–240. Academic Press, London.
47. Gu L, Baldocchi DD, Wofsy SC, Munger JW, Michalsky JJ, et al. (2003) Response of a deciduous forest to the Mount Pinatubo eruption: enhanced photosynthesis. *Science* 299: 2035–2038.
48. Urban O, Janouš D, Acosta M, Czerný R, Marková I, et al. (2007) Ecophysiological controls over the net ecosystem exchange of mountain spruce stand. Comparison of the response in direct vs. diffuse solar radiation. *Global Change Biol* 13: 157–168.
49. Kuiper PJC (1964) Dependence upon wavelength of stomatal movement in epidermal tissue of *Senecio odoris*. *Plant Physiol* 39: 952–955.
50. Mansfield TA, Meidner H (1966) Stomatal opening in light of different wavelengths: effects of blue light independent of carbon dioxide concentration. *J Exp Bot* 17: 510–521.
51. Morison JIL, Jarvis PG (1983) Direct and indirect effects of light on stomata. I. In Scots pine and Sitka spruce. *Plant Cell Environ* 6: 95–101.
52. Karlsson PE (1986) Blue light regulation of stomata in wheat seedlings. II. Action spectrum and search for action dichroism. *Physiol Plant* 66: 207–210.
53. Pejam MR, Arain MA, McCaughey JH (2006) Energy and water vapour exchanges over a mixedwood boreal forest in Ontario, Canada. *Hydrol Process* 20: 3709–3724.
54. Aphalo PJ, Jarvis PG (1993) Separation of direct and indirect responses of stomata to light: results from a leaf inversion experiment at constant intercellular CO₂ molar fraction. *J Exp Bot* 44: 791–800.
55. Matsuda R, Ohashi-Kaneko K, Fujiwara K, Goto E, Kurata K (2004) Photosynthetic characteristics of rice leaves grown under red light with or without supplemental blue light. *Plant Cell Physiol* 45: 1870–1874.